

Computational Graph Approach for Detection of Composite Human Activities

Niko Reunanen, Ville Könönen, Hermanni Hälvä, Jani Mäntyjärvi, Arttu Lämsä and Jussi Liikka

Abstract—Existing work in human activity detection classifies physical activities using a single fixed-length subset of a sensor signal. However, temporally consecutive subsets of a sensor signal are not utilized. This is not optimal for classifying physical activities (composite activities) that are composed of a temporal series of simpler activities (atomic activities). A sport consists of physical activities combined in a fashion unique to that sport. The constituent physical activities and the sport are not fundamentally different. We propose a computational graph architecture for human activity detection based on the readings of a triaxial accelerometer. The resulting model learns 1) a representation of the atomic activities of a sport and 2) to classify physical activities as compositions of the atomic activities. The proposed model, alongside with a set of baseline models, was tested for a simultaneous classification of eight physical activities (walking, Nordic walking, running, soccer, rowing, bicycling, exercise bicycling and lying down). The proposed model obtained an overall mean accuracy of 77.91% (population) and 95.28% (personalized). The corresponding accuracies of the best baseline model were 73.52% and 90.03%. However, without combining consecutive atomic activities, the corresponding accuracies of the proposed model were 71.52% and 91.22%. The results show that our proposed model is accurate, outperforms the baseline models and learns to combine simple activities into complex activities. Composite activities can be classified as combinations of atomic activities. Our proposed architecture is a basis for accurate models in human activity detection.

Keywords—Activity recognition, computational graph

I. INTRODUCTION

Human activity detection is the process of classifying the current physical activity of a person. A common data source for human activity detection is instantaneous acceleration (used in [1], [2], [3], [4], [5], [6], [7], [8]). Accelerometers are lightweight [9], inexpensive [10], and widely available [11] across wrist devices and smart phones [8], and thus any built-in system could be distributed broadly.

Arguably, some physical activities are more complex than others in that they consist of other, more fundamental, sub-activities. We introduce the following terms: composite activities and atomic activities. Each composite activity is a unique temporal series of consecutive atomic activities. Therefore the atomic activities are building blocks for defining complex activities. Some sports are complex activities (e.g. basketball)

that are combinations of constituent physical activities (atomic activities). Notice that simple activities are also defined as composite activities in which consecutive atomic activities are almost identical.

Previous work in human activity detection typically consists of the following steps: aggregation of a subset of a sensor signal, summarization of the information in the subset (e.g. sample statistics) and an instantaneous classification of the physical activity (used in [4], [8], [12], [13]). Models that utilize the previous three steps face a fundamental problem in classifying composite activities. For instance, the act of playing basketball includes running, and thus these models may struggle to learn separate representations for them. Our proposed model enables the detection of such complex physical activities by first decomposing them into unique atomic activities (Section II-B) and then combining these for activity classification (Section II-C).

In this paper, we propose a model for classifying the physical activity of a person based on the readings of a triaxial accelerometer. Compared to the existing work, our model has the following benefits:

- The model learns to classify the physical activities as composite activities, which consist of atomic activities.
- The computed features, which characterize the atomic activities and the composite activities, are not selected from a fixed set of features (e.g. mean or variance, as in [4], [8]). Instead, the features are learned automatically to represent the supported physical activities. Therefore we do not impose assumptions on how to build a representation of the subsets of a sensor signal to summarize their information.
- The model can be utilized as a population system and as a personalized system. For a test subject, a population system is created using data of other people and a personalized system is created using data of the test subject. Our proposed model is used to experiment with both systems in Section III.

The proposed model is trained end-to-end as a single model without manual intervention. The computational components of our model originate from deep learning literature [14]. However, the model uses a limited amount of memory and is not a deep model. Instead, one should consider our model to be a computational graph [15], [16].

The experiments in this paper use a total of six hours of data from Palantir Context Data Library [12], [13]. This data was created by recording multiple sensors, including a triaxial wrist-worn accelerometer, while users performed various activities. The sampling frequency of the accelerometer

N. Reunanen, V. Könönen, J. Mäntyjärvi, A. Lämsä and J. Liikka are with the VTT Technical Research Centre of Finland, Kaitoväylä 1, 90571, Oulu, Finland. E-mail: niko.reunanen@vtt.fi, ville.kononen@vtt.fi, jani.mantyljarvi@vtt.fi, arttu.lamsa@vtt.fi, jussi.liikka@vtt.fi.

H. Hälvä is with the VTT Technical Research Centre of Finland, Tekniikkatie 1, 02150, Espoo, Finland. E-mail: hermanni.halva@vtt.fi.

was 20Hz, which is sufficient to detect physical activities [4]. The data were recorded outside a laboratory in a real-world environment, and represent a set of activities, which are performed in personal ways (e.g. two persons run in different ways.) Therefore, by utilizing the Palantir data, we obtain a good estimate of the real-world accuracy of our model for human activity detection. See [12], [13] for a detailed description of the data and the setup of the data collection.

The scope of our work in this paper is in the classification of eight physical activities (walking, Nordic walking, running, soccer, rowing, bicycling, exercise bicycling and lying down). A physical activity is classified using a subset of 15 seconds of acceleration signal. We also construct and evaluate a set of baseline models to classify the 15s of acceleration signal. The following established classifiers are selected as the baseline models in the experiments: logistic regression [17], random forest classifier [18], decision tree [17], adaptive boosting classifier [19] and linear support vector machine [17]. The proposed model obtained an overall mean accuracy of 77.91% (population) and 95.28% (personalized). The corresponding accuracies of the best baseline model (random forest) were 73.52% and 90.03%.

The reported parametrization of our proposed model in this paper (e.g. the number of computational units) was selected through empirical experiments. Our goal is not to provide a universal and general parametrization for the model. However, the parametrization utilized in this paper is a solid initial choice, which is experimentally validated. Rather, our goal is to introduce a suitable architecture for a model to detect composite activities. The following section defines the architecture and its parametrization used in this paper.

II. THE PROPOSED MODEL

To detect composite activities, we propose a model with three major components:

- 1) Feature learning for atomic activities (Section II-B).
- 2) Feature learning for a composite activity (Section II-C).
- 3) Classification of the composite activity (Section II-D).

An atomic activity is encoded into a vector of real values, which encode its characteristics. These values are called features and the process of learning to compute them is called feature learning (see Section II-B). A set of feature vectors, corresponding to atomic activities, is sent to a recurrent model which is used as it is able to learn the temporal relationship between these features [20]. The final internal state of the recurrent model, which is a vector of real values, represents the feature values of the composite activity. Therefore the representation of a composite activity is learned using the atomic activities (see Section II-C). The final internal state is then classified into one of the supported physical activities (see Section II-D). The following subsection introduces the computational machinery, which are then examined in further detail in sections II-B, II-C and II-D.

A. Computation in layers

We factor the computation of our proposed model into consecutive steps called layers. A layer takes an input, transforms the input and outputs the transformed value. A set of

chained layers forms a computational graph. For example, neural networks can be defined as computational graphs. The following layers are utilized by our model (see [14], [20], [21], [22], [23] for more details):

- Fully connected layer (FC). The layer applies a non-linear function element-wise to an affine transformation: $\sigma(\mathbf{W}\mathbf{x} + \mathbf{b})$ where $\mathbf{x} \in \mathbb{R}^d$ denotes d -dimensional input and \mathbf{W}, \mathbf{b} are adjustable parameters. We utilize a rectified linear unit for the non-linearity ($\sigma(a) = \max(0, a)$), which is widely employed as the non-linearity [21] because of its calculational simplicity [24]. We use fully connected layers to learn suitable features to classify the physical activities.
- Convolution layer (CO). The layer processes an input signal while retaining its temporal structure. Similarly to a FC layer, a convolution layer applies affine transformations followed by a non-linearity. The parameters for affine transformations are contained in convolution kernels. The same convolution kernel parameters are used across all the temporal subsets of the input signal. Each convolution kernel in each layer outputs a new transformed signal. Convolution layers can use multiple convolution kernels to output multiple transformed signals. The goal is to learn translation invariant features (kernels) from the input signal.
- Max-pooling layer (MP). This layer reduces the dimensionality of its input signal by outputting only the largest input value from temporally neighboring regions. The size of a region is four without overlapping in our experiments. Therefore, for example, eight temporally consecutive acceleration readings are transformed into two values.
- Long short term memory layer (LSTM). LSTM is a specific type of a recurrent neural network, which utilizes a gating mechanism to retain an internal state over a long period of time in its memory [20]. During every time step, the LSTM determines its internal state based on the current input vector (atomic feature vector) and its own previous state. Each composite activity is modeled using the final state of the LSTM.
- Softmax layer (SM). The layer computes a probability distribution (relative probabilities) for the physical activities as $P(i) = e^{z_i} (\sum_{j=1}^8 e^{z_j})^{-1}$ where $P(i)$ is the probability of i :th activity and z_i is the i :th input value for the layer. We use a softmax layer, and the resulting probability distribution, to predict the current physical activity.

The layers compute the gradient of their parameters with respect to its output (e.g. $\frac{\partial \sigma}{\partial \mathbf{W}} = \frac{\partial \sigma}{\partial a} \frac{\partial a}{\partial \mathbf{W}}$, $\frac{\partial \sigma}{\partial \mathbf{b}} = \frac{\partial \sigma}{\partial a} \frac{\partial a}{\partial \mathbf{b}}$ and $\frac{\partial \sigma}{\partial \mathbf{x}} = \frac{\partial \sigma}{\partial a} \frac{\partial a}{\partial \mathbf{x}}$ for FC). The gradient between consecutive layers is computed using the chain rule where the gradient of the lower layer is multiplied by the gradient of the upper layer. This allows one to compute the gradient of all parameters with respect to the desired output of the computational graph.

The deviation between the desired output (y) and the output of the computational graph (\hat{y}) is measured using an error function ($e(y, \hat{y})$). The final layer in our model is a softmax

layer, which forms a probability distribution of the classification results. Therefore we obtain the probabilities of the eight physical activities. The classification result is the physical activity with the highest probability. The error function is the cross-entropy function between the computed probability distribution and the desired probability distribution, see [25] for details. To minimize the error function, the parameter values are updated using gradient descent as:

$$\Theta = \Theta - \alpha * \frac{\partial e}{\partial \Theta}, \quad (1)$$

where Θ is the set of model parameters and $\alpha \in \mathbb{R}$ is a hyperparameter called learning rate. The learning rate scales the magnitude of the gradient descent [17]. It is important to select an appropriate value of the learning rate for the convergence of the model. Section II-E explains the training procedure of our proposed model in detail. The computational graph is trained by minimizing the error function. This approach is known as the backpropagation algorithm in the neural network literature, see [25], [17], [26] for more details. The following subsection describes the feature learning for atomic activities in detail.

B. Feature learning for atomic activities

An atomic activity is represented as a d -dimensional vector of real values ($\mathbf{x} \in \mathbb{R}^d$). We selected $d = 128$ based on empirical tests using the values $d \in \{8, 16, 32, 64, \dots, 512\}$. The input for computing \mathbf{x} in our experiments is three seconds of sensor signal from a triaxial accelerometer (three axes, 20Hz sampling rate.) Feature learning ($f : \mathbb{R}^{3 \times 3 \times 20} \rightarrow \mathbb{R}^d$) transforms the acceleration signal into a feature representation of a fixed size (d).

Fig. 1 illustrates the architecture of the computational graph for learning and computing the features of an atomic activity (AFL). The computation of the features commences by processing the acceleration signal in two consecutive convolution layers. The convolution kernels learn to identify signal patterns that correspond to different atomic activities. We experimented using a various number of consecutive convolution layers (architecture) and kernels (parametrization). We utilize two layers with 8 and 32 kernels because they provided good results consistently. The maximum values of the twice convolved signal are pooled to reduce the number of parameters. The final layer is a fully connected layer, which acquires the pooled signal. The outputs of the fully connected layer are the feature values (\mathbf{x}) of an atomic activity. A larger model (see Fig. 2) utilizes these feature values (Fig. 1) to learn a composite activity from atomic activities. The following subsection describes the feature learning for composite activities in detail.

C. Feature learning for composite activities

In our experiments, a composite activity is segmented into five consecutive atomic activities, which results in a total of 15 seconds of acceleration signal. Using the feature learning for atomic activities (AFL) in Fig. 1, the atomic activities are transformed into five vectors of feature values ($\mathbf{x}_1, \mathbf{x}_2, \mathbf{x}_3, \mathbf{x}_4, \mathbf{x}_5$). The parametrization of AFL is shared across the temporally

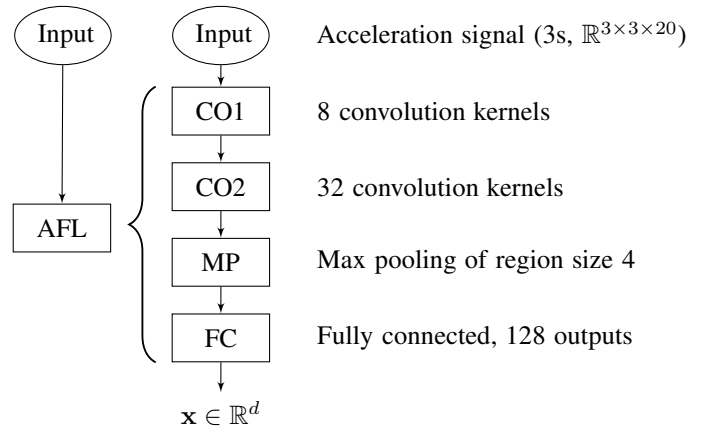


Fig. 1: An illustration of a computational graph for the feature learning for atomic activities (AFL). The features are encoded as a vector of 128 values ($\mathbf{x} \in \mathbb{R}^d, d = 128$), which are computed by the fully connected layer (FC). The input data ($\mathbb{R}^{3 \times 3 \times 20}$) contain three seconds of acceleration signal from a triaxial accelerometer with a sampling rate of 20Hz.

consecutive subsets (3s) of the acceleration signal. The feature vectors are provided to LSTM, one vector at a time in temporal order. The final internal state of LSTM (s_5) is the feature representation of the composite activity, which encodes the composite activity using the atomic activities. Fig. 2 illustrates the feature learning for composite activities. The following subsection describes how to classify the current physical activity of a person given the final internal state of the LSTM.

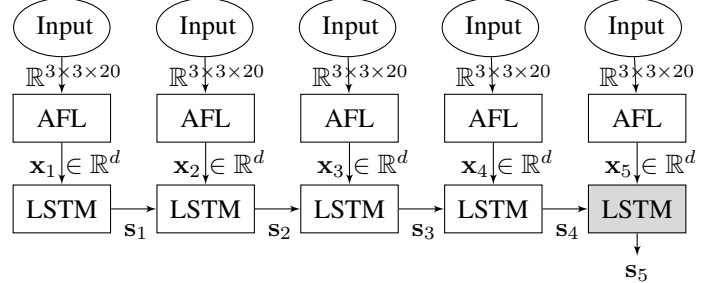


Fig. 2: A composite activity is a temporal series of consecutive atomic activities, which are represented by feature values (\mathbf{x}_i^d). Long Short Term Memory obtains \mathbf{x}_i^d chronologically one at a time to learn the temporal relationships between the atomic activities. The internal states of the LSTM (s_i) are a representation of a composite activity, which is updated internally (arrows between LSTM blocks) and by the atomic activities (arrows from feature learning). The final internal state of the LSTM (s_5) is the feature representation of the composite activity.

D. Classification of the composite activities

In order to classify the current physical activity, the feature representation of a composite activity (s_5 in Fig. 2) is passed through two fully connected layers. The second fully connected layer outputs a vector, with a dimensionality that matches the number of supported physical activities. This vector is

then transformed into a probability distribution by a softmax layer, and the classification result is the physical activity that corresponds to the highest relative probability. This process is depicted in Fig. 3. The next section describes the setup of the experiments and reports the obtained results.



Fig. 3: The physical activity is classified using the final internal state (s_5) from the LSTM (see Fig. 2). The first fully connected layer (FC1) transforms s_5 into a fixed-size representation to suit the classification task. The second fully connected layer (FC2) transforms the output of FC1 into a vector of dimensionality matching the number of supported physical activities. The softmax layer (SM) transforms the output of FC2 into a probability distribution over the physical activities. The classification result is the physical activity with the highest probability.

E. Training the model

Our model is trained using the established backpropagation algorithm (applied recently in [27], [28], [29], [30].) The convergence of the backpropagation is affected by the selection of a suitable learning rate (α in Eq. 1) [23]. We apply Adam algorithm [31] for adaptive selection of the learning rate (used in [32], [33], [34]), which does not require an initial selection of a fixed learning rate. We evaluated empirically that the model converged significantly faster using Adam than with a fixed learning rate (stochastic gradient descent). Adam converges fast because 1) it calculates a separate learning rate for each of the features in the model and 2) it incorporates momentum in the gradient descent. See [17] for details.

The model parametrization used in this paper requires a high number of adjustable parameters (278 696). One challenge with the model is its tendency to overfit the training data; that is, it does not generalize well with previously unseen data [22], [17], [27], [35]. One indicator of an overfitted model is a large norm of weight parameters [17]. If the weight values are large in the inner product (e.g. \mathbf{W} in $\sigma(\mathbf{W}\mathbf{x} + \mathbf{b})$), then small changes in the input cause large changes in the value of the inner product. A model becomes overly specific to the training data with large values of \mathbf{W} . To improve the generalization ability, we utilize L_2 regularization in the weight values of the fully connected layers, the LSTM and the convolution layers. The L_2 regularization penalizes the training of the model with a specified regularization strength (γ) as $L_2(\mathbf{W}, \gamma) = \gamma \sum_i W_i^2$ where $\sum_i W_i^2$ is the sum of the squared weight values [17] and $\mathbf{W} \in \Theta$. In our experiments, we use the regularization strength of $\gamma = 0.01$.

To further improve the generalization ability and to reduce overfitting, we employ a technique called dropout [27]. We use dropout to randomly disable portions of inputs in the fully connected layers and the LSTM with 50% probability as in [22]. Therefore our model has to learn a robust classification as the model cannot rely on having an access to all of the available information. Dropout forces the computational units to rely on themselves, and not to co-adapt with each other, which

improves the classification accuracy of the neural network [22], [27].

Despite the L_2 regularization and dropout, we observed overfitting because 1) the representational capacity of the model is high and 2) Adam is an efficient method for stochastic optimization. In the experiments in Section III, our model consistently provided good results in the beginning of the training procedure. Therefore we utilized an approach called early stopping that trains a model for a limited amount of time. In our experiments, the training was stopped after two iterations of the gradient descent (Eq. 1) using Adam algorithm. See [17], [36], [37] for a detailed definition of the early stopping. The following section describes the evaluation experiments and reports their results.

III. EXPERIMENTS

The experiments use data recorded on nine persons. The data originate from the Palantir Context Data Library, see [12], [13] for more details. It consists of five minutes of acceleration signal for the following physical activities: walking, Nordic walking, running, soccer, rowing, bicycling, exercise bicycling and lying down. The data were recorded using a triaxial accelerometer worn on the wrist. Two types of experiments are conducted for each test subject: a population system and a personalized system. The resulting classification accuracies are then reported. A population system is created using 40 minutes of acceleration signal (from 8 test subjects) and evaluated using 5 minutes of acceleration signal (from one test subject). This simulates a use-case where a user utilizes a previously created model for human activity detection. A personalized system is constructed for each test subject using the first two minutes of the acceleration signal per physical activity. The classification accuracy is evaluated using the remaining three minutes of the acceleration signal. This simulates a use-case where the user of the system creates a personalized model for human activity detection from scratch.

The following established classifiers are selected as the baseline models in the experiments: logistic regression [17], random forest classifier [18], decision tree [17], adaptive boosting classifier [19] and linear support vector machine [17]. Gaussian support vector machine is not selected because of its infeasible computation time. The baseline models utilize the data in one go (15 seconds of acceleration signal). We train, evaluate and report the baseline models individually. The next subsection reports the results from the experiments. The baseline models do not model the physical activities as combinations of composite activities. Instead, like in the existing work [4], [8], [12], [13], the baseline models attempt to instantaneously determine the current physical activity.

A. Results using a population model

A population system was constructed for each test subject using our proposed model and the baseline models. For example, for the first test subject, a population system was constructed using the data from the remaining (eight) test subjects. The experiments measure the effectiveness of providing a pre-existing, non-personalized model for human

activity detection. Table I reports the mean accuracies for the population systems by repeating their construction and evaluation ten times. The proposed model obtained an overall mean accuracy of 77.91%, while the best baseline model (random forest) obtained an overall mean accuracy of 73.52%. The proposed model also provides the highest mean accuracy for the individual users. Compared to the the best baseline model, significant improvements in the mean accuracies are obtained using the proposed model for users one (95.26% vs 90.65%), three (95.65% vs 91.91%) and eight (81.72% vs. 71.53%). The results show that our model outperforms the baseline models.

The models do not provide good results for the fifth and the sixth user. This unveils a fundamental problem with the population system; it cannot recognize an activity if a user performs it in a personal, unique, manner. For users five and six, soccer consisted of significant amounts of walking and lying down, and hence the model had trouble distinguishing soccer from the latter two, hence the low accuracies. The following subsection reports results from experiments where the users are provided a personalized system.

B. Results using a personalized model

A personalized system was constructed for each test subject using our proposed model and the baseline models. Table II reports the mean accuracies for the personalized systems by repeating their construction and evaluation ten times. The mean accuracy of our model exceeds 90% for the users while the baseline models are accurate for a subset of the users. The overall mean accuracy of the proposed model is 95.28%, while the best baseline model (random forest) obtained an overall mean accuracy of 90.03%. The proposed model also provides the highest mean accuracy for the individual users. The results show that our model outperforms the baseline models.

As explained above, human activity detection for the user 5 is particularly challenging as physical activities are not well defined. However, our model learns the composite activity of soccer for the user 5, which is one of the advantages of the personalized system. The mean accuracy is 92.03% using the proposed model. The baseline models do not model physical activities explicitly as composite activities, which results in significantly lower accuracies than those of our model. The best baseline model obtained a mean accuracy of 76.07%. Therefore it is beneficial to use our model when the physical activities are difficult to classify without considering the temporal series of atomic activities.

IV. IMPORTANCE OF THE COMPOSITE ACTIVITIES

The central assumption of our work is that composite activities are efficiently learned as temporal series of atomic activities. To explicitly study the validity of this assumption, we conducted two experiments in the following two subsections.

A. Human activity detection without composite activities

We removed the recurrent components (Fig. 2) from the proposed model to test the importance of the composite activities. The trimmed model, which does not explicitly combine

the atomic activities in time, is illustrated in Fig. 4. The input for the model is 15s of acceleration signal in one go.



Fig. 4: A trimmed version of the proposed model where components for combining atomic activities (Fig. 2) are removed. The resulting model tests the impact on accuracy of not combining atomic activities into composite activities.

The trimmed model was utilized as a population system and a personalized system for the nine users. Table III reports the mean accuracies (ten repetitions) for the trimmed model, as well as the full model, for comparison. The full model provides a better performance for the users with mean accuracies of 77.9% in the population system and 95.3% in the personalized system. The respective figures for the trimmed model are 71.52% and 91.22%, respectively. The results suggest that the utilization of composite activities improves the accuracy of human activity detection.

B. Visualization of the recurrent states

We projected the first and the last internal states of the LSTM (s_1 and s_5 in Fig. 2) into a two-dimensional manifold. The projection was computed using t-distributed stochastic neighbor embedding (t-SNE, [38], [39]), which is designed to visualize high-dimensional data. The internal LSTM states of a personalized model for the second test subject were computed using three minutes of validation data. Fig. 5 illustrates the obtained results using t-SNE where the left image is the first internal state and the right image is the last internal state. Notice that initially some of the composite activities are mixed with atomic activities. For example, soccer overlaps with walking and running. This suggests that it is a fundamentally challenging task to instantaneously recognize composite activities. However, walking and running do not overlap with soccer in the last internal state of the LSTM. Therefore our model has learned to identify composite activities as temporal series of atomic activities.

V. DISCUSSION AND CONCLUSION

There are complex activities (composite activities) that consist of simpler activities (atomic activities). It is a fundamentally challenging task to classify a composite activity without decomposing it into atomic activities. In this paper, we have proposed a model to automatically learn the atomic activities and how to combine them into composite activities. The experiments in Section III show the following benefits of our model:

- 1) Our proposed model learns to form a set of atomic activities and to combine them meaningfully. Instantaneous classification is not sufficient and one needs to learn the composite activities as combinations of atomic activities over time. This is suggested from inspecting Fig. 5 and the results in Table III.

	User 1	User 2	User 3	User 4	User 5	User 6	User 7	User 8	User 9	Mean
Proposed	0.9526	0.9454	0.9565	0.8325	0.3985	0.3862	0.8403	0.8172	0.8824	0.7791
Logistic regression	0.5540	0.6319	0.5549	0.6274	0.2113	0.2916	0.5379	0.3617	0.6215	0.4880
Random forest	0.9065	0.9390	0.9191	0.8049	0.3595	0.2973	0.8096	0.7153	0.8659	0.7352
Decision tree	0.8402	0.7854	0.7946	0.6982	0.3304	0.3089	0.6836	0.6055	0.7235	0.6411
Adaptive boosting	0.4918	0.4602	0.5164	0.5671	0.0925	0.3376	0.5319	0.4115	0.4514	0.4289
Linear support vector machine	0.5361	0.5626	0.5403	0.4033	0.1364	0.3516	0.4405	0.3958	0.4618	0.4254

TABLE I: Results using a population system. The cells denote the mean classification accuracies (ten repetitions) for our proposed model and the baseline models. The last column denotes the mean accuracy over all users. The best results are bolded. Our proposed model outperforms the baseline models. Significant benefits are obtained for users 1, 3 and 8 using our proposed model.

	User 1	User 2	User 3	User 4	User 5	User 6	User 7	User 8	User 9	Mean
Proposed	0.9974	0.9784	0.9857	0.9334	0.9203	0.9278	0.9422	0.9065	0.9836	0.9528
Logistic regression	0.8602	0.8705	0.9304	0.8435	0.6907	0.9045	0.7999	0.6099	0.8669	0.8196
Random forest	0.9964	0.8880	0.9855	0.9059	0.7607	0.8943	0.8523	0.8979	0.9221	0.9003
Decision tree	0.9076	0.8130	0.8939	0.8087	0.6890	0.8412	0.7367	0.7437	0.8470	0.8090
Adaptive boosting	0.4499	0.3207	0.5384	0.2753	0.2215	0.2714	0.4878	0.2707	0.7051	0.3934
Linear support vector machine	0.8690	0.8037	0.8804	0.8145	0.5923	0.8949	0.7896	0.6378	0.8449	0.7919

TABLE II: Results using a personalized system. The cells denote the mean classification accuracies (ten repetitions) for our proposed model and the baseline models. The last column denotes the mean accuracy over all users. The best results are bolded. Our proposed model outperforms the baseline models by providing a mean accuracy over 90% for the users. The baseline models are efficient only for a subset of the users. Compared to the baseline models, users 5, 7 and 9 obtain significantly better results using our proposed model.

	User 1	User 2	User 3	User 4	User 5	User 6	User 7	User 8	User 9	Mean
Population (full)	0.9526	0.9454	0.9565	0.8325	0.3985	0.3862	0.8403	0.8172	0.8824	0.7791
Population (trimmed)	0.8290	0.8997	0.8546	0.8204	0.2896	0.3829	0.8257	0.7234	0.8112	0.7152
Personalized (full)	0.9974	0.9784	0.9857	0.9334	0.9203	0.9278	0.9422	0.9065	0.9836	0.9528
Personalized (trimmed)	0.9662	0.9222	0.9775	0.8985	0.7898	0.9120	0.9405	0.8255	0.9776	0.9122

TABLE III: Population and personalized system results for the trimmed and full version of the proposed model. The trimmed version does not combine atomic activities in time. The cells denote the mean classification accuracies (ten repetitions). The last column denotes the mean accuracy over all users. The best results are bolded. Compared to the trimmed version of the model, the full version provides a higher accuracy for the users. The results suggest that it is beneficial for human activity detection to combine atomic activities into composite activities.

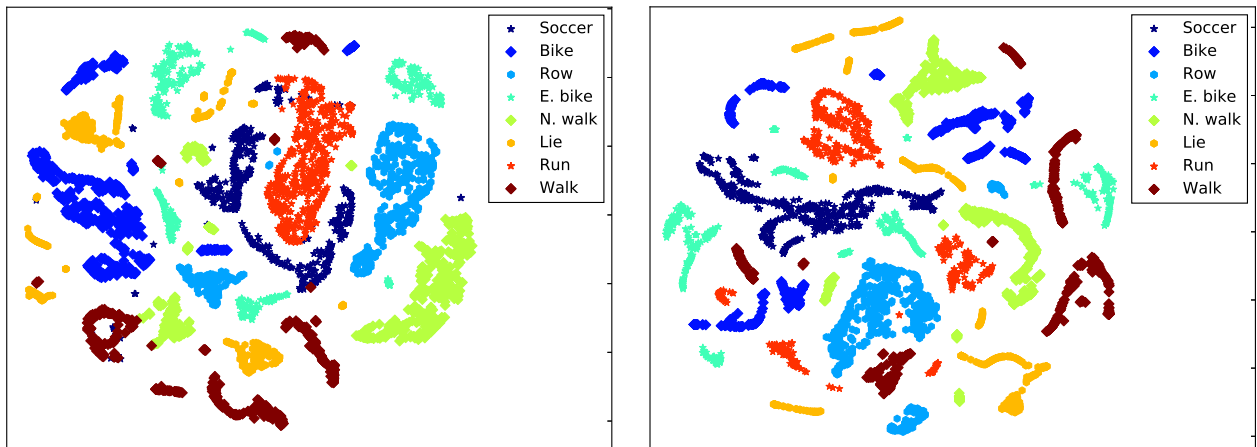


Fig. 5: Visualization of the internal states of the LSTM (s_t in Fig. 2) per physical activity for the second test subject. Best viewed in color. The internal states are projected in a two-dimensional manifold using t-SNE algorithm. **Left:** The first internal state (s_1 in Fig. 2.) **Right:** The final internal state (s_5 in Fig. 2.) Notice that the composite activities can overlap with related atomic activities (e.g. soccer, walking and running overlap) in the first internal state. However, using s_5 , all of the physical activities are separated from each other and the clusters are more compact.

- 2) The proposed model outperforms the baseline models by obtaining an overall mean accuracy of 77.91% (population) and 95.28% (personalized). The corresponding accuracies of the best baseline model were 73.52% and 90.03%. However, the corresponding accuracies of the proposed model without utilizing the composite activities was 71.52% and 91.22%.

The limitations of our model are the utilization of 15s of acceleration signal and the memory consumption. Depending on the application domain, 15 seconds can be adequate. However, our model is not suited for time-critical systems that require a low latency for the results. Additionally, the current parametrization of our model uses 8.92Mb (32bit floating point values) of memory. This can be a large amount of memory for small embedded devices. One of our goals is to find a small parametrization, which retains a good accuracy. However, we believe that the amount of available device memory is going to increase. Future work includes the following:

- Further experiments using different parametrizations of the proposed model.
- Unsupervised segmentation of acceleration signal using the learned features in Fig. 2 and 3.
- Fusion of different sensor signals for human activity detection.

REFERENCES

- [1] J. Mäntyjärvi, J. Himberg, and T. Seppänen, "Recognizing human motion with multiple acceleration sensors," in *Proceedings of the 2001 IEEE International Conference on Systems, Man, and Cybernetics*, vol. 2, 2001, pp. 747–752.
- [2] M. Mathie, B. Celler, N. Lovell, and A. Coster, "Classification of basic daily movements using a triaxial accelerometer," *Medical and Biological Engineering and Computing*, vol. 42, no. 5, pp. 679–687, 2004.
- [3] D. M. Karantonis, M. R. Narayanan, M. Mathie, N. H. Lovell, and B. G. Celler, "Implementation of a real-time human movement classifier using a triaxial accelerometer for ambulatory monitoring," *IEEE Transactions on Information Technology in Biomedicine*, vol. 10, no. 1, pp. 156–167, Jan. 2006.
- [4] P. Gupta and T. Dallas, "Feature selection and activity recognition system using a single triaxial accelerometer," *IEEE Transactions on Biomedical Engineering*, vol. 61, no. 6, pp. 1780–1786, June 2014.
- [5] A. Khan, Y. Lee, S. Lee, and T. Kim, "A triaxial accelerometer-based physical-activity recognition via augmented-signal features and a hierarchical recognizer," *IEEE Transactions on Information Technology in Biomedicine*, vol. 14, no. 5, pp. 1166–1172, Sep 2010.
- [6] S. Chernbumroong, A. Atkins, and H. Yu, "Activity classification using a single wrist-worn accelerometer," in *Proceedings of the 2011 5th International Conference on Software, Knowledge Information, Industrial Management and Applications (SKIMA)*, Sept 2011, pp. 1–6.
- [7] A. Godfrey, A. Bourke, G. Olaighin, P. van de Ven, and J. Nelson, "Activity classification using a single chest mounted tri-axial accelerometer," *Medical Engineering & Physics*, vol. 33, pp. 1127–1135, 2011.
- [8] J. Kwapisz, G. Weiss, and S. Moore, "Activity recognition using cell phone accelerometers," *SIGKDD Explor. Newsl.*, vol. 12, no. 2, pp. 74–82, Mar 2011.
- [9] J. Petersen, D. Austin, R. Sack, and T. Hayes, "Actigraphy-based scratch detection using logistic regression," *IEEE Journal of Biomedical and Health Informatics*, vol. 17, no. 2, pp. 277–283, Mar 2013.
- [10] W. Cheng and D. Jhan, "Triaxial accelerometer-based fall detection method using a self-constructing cascade-adaboost-svm classifier," *IEEE Journal of Biomedical and Health Informatics*, vol. 17, no. 2, pp. 411–419, Mar 2013.
- [11] A. Matic, V. Osmani, and O. Mayora, "Speech activity detection using accelerometer," in *Proceedings of the 2012 IEEE Annual International Conference on Engineering in Medicine and Biology Society*, Aug 2012, pp. 2112–2115.
- [12] J. Pärkkä, M. Ermes, P. Korpijärvi, J. Mäntyjärvi, J. Peltola, and I. Korhonen, "Activity classification using realistic data from wearable sensors," *IEEE Transactions on Information Technology in Biomedicine*, vol. 10, no. 1, pp. 119–128, Jan. 2006.
- [13] M. Ermes, J. Pärkkä, J. Mäntyjärvi, and I. Korhonen, "Detection of daily activities and sports with wearable sensors in controlled and uncontrolled conditions," *IEEE Transactions on Information Technology in Biomedicine*, vol. 12, no. 1, pp. 20–26, Jan. 2008.
- [14] J. Schmidhuber, "Deep learning in neural networks: An overview," *Neural Networks*, vol. 61, pp. 85–117, 2015.
- [15] D. Koller and N. Friedman, *Probabilistic Graphical Models: Principles and Techniques - Adaptive Computation and Machine Learning*. The MIT Press, 2009.
- [16] F. Bastien, P. Lamblin, R. Pascanu, J. Bergstra, I. Goodfellow, A. Bergeron, N. Bouchard, and Y. Bengio, "Theano: new features and speed improvements," in *Deep Learning and Unsupervised Feature Learning NIPS 2012 Workshop*, 2012.
- [17] C. Bishop, *Pattern Recognition and Machine Learning*. Secaucus, NJ, USA: Springer-Verlag New York, Inc., 2006.
- [18] L. Breiman, "Random forests," *Machine learning*, vol. 45, no. 1, pp. 5–32, Oct 2001.
- [19] Y. Freund and R. Schapire, "Experiments with a new boosting algorithm," in *Proceedings of the Thirteenth International Conference on Machine Learning (ICML 1996)*, L. Saitta, Ed. Morgan Kaufmann, 1996, pp. 148–156.
- [20] S. Hochreiter and J. Schmidhuber, "Long short-term memory," *Neural Computing*, vol. 9, no. 8, pp. 1735–1780, Nov 1997.
- [21] Y. LeCun, Y. Bengio, and G. Hinton, "Deep learning," *Nature*, pp. 436–444, 2015.
- [22] A. Krizhevsky, I. Sutskever, and G. Hinton, "Imagenet classification with deep convolutional neural networks," in *Advances in Neural Information Processing Systems 25*, F. Pereira, C. Burges, L. Bottou, and K. Weinberger, Eds. Curran Associates, Inc., 2012, pp. 1097–1105.
- [23] Y. Bengio, *Neural Networks: Tricks of the Trade: Second Edition*. Berlin, Heidelberg: Springer Berlin Heidelberg, 2012, ch. Practical Recommendations for Gradient-Based Training of Deep Architectures, pp. 437–478.
- [24] X. Glorot, A. Bordes, and Y. Bengio, "Deep sparse rectifier neural networks," in *Proceedings of the Fourteenth International Conference on Artificial Intelligence and Statistics*, vol. 15, 2011, pp. 315–323.
- [25] S. Theodoridis and K. Koutroumbas, *Pattern Recognition*, 4th ed. Academic Press, 2008.
- [26] T. Mitchell, *Machine Learning*, 1st ed. New York, NY, USA: McGraw-Hill, Inc., 1997.
- [27] N. Srivastava, G. Hinton, A. Krizhevsky, I. Sutskever, and R. Salakhutdinov, "Dropout: A simple way to prevent neural networks from overfitting," *Journal of Machine Learning Research*, vol. 15, pp. 1929–1958, 2014.
- [28] I. Goodfellow, J. Pouget-Abadie, M. Mirza, B. Xu, D. Warde-Farley, S. Ozair, A. Courville, and Y. Bengio, "Generative adversarial nets," in *Advances in Neural Information Processing Systems 27*. Curran Associates, Inc., 2014, pp. 2672–2680.
- [29] Y. Li, K. Swersky, and R. Zemel, "Generative moment matching networks," in *ICML*, ser. JMLR Proceedings, F. Bach and D. Blei, Eds., vol. 37, 2015, pp. 1718–1727.
- [30] N. Srivastava and R. Salakhutdinov, "Multimodal learning with deep

- boltzmann machines,” in *Advances in Neural Information Processing Systems 25*. Curran Associates, Inc., 2012, pp. 2222–2230.
- [31] D. Kingma and J. Ba, “Adam: A method for stochastic optimization,” *CoRR*, vol. abs/1412.6980, 2014.
- [32] J. Chung, K. Kastner, L. Dinh, K. Goel, A. Courville, and Y. Bengio, “A recurrent latent variable model for sequential data,” in *Advances in Neural Information Processing Systems 28: Annual Conference on Neural Information Processing*, 2015, pp. 2980–2988.
- [33] A. Rasmus, H. Valpola, M. Honkela, M. Berglund, and T. Raiko, “Semi-supervised learning with ladder networks,” in *Proceedings of the 28th International Conference on Neural Information Processing Systems*, ser. NIPS’15, 2015, pp. 3546–3554.
- [34] K. Gregor, I. Danihelka, A. Graves, D. Rezende, and D. Wierstra, “Draw: A recurrent neural network for image generation,” in *Proceedings of the 32nd International Conference on Machine Learning (ICML-15)*. JMLR Workshop and Conference Proceedings, 2015, pp. 1462–1471.
- [35] K. P. Murphy, *Machine Learning: A Probabilistic Perspective*. The MIT Press, 2012.
- [36] L. Prechelt, “Early stopping but when?” in *Neural Networks: Tricks of the Trade*, ser. Lecture Notes in Computer Science, 2012, vol. 7700.
- [37] D. Barber, *Bayesian Reasoning and Machine Learning*. New York, NY, USA: Cambridge University Press, 2012.
- [38] L. Van Der Maaten and G. Hinton, “Visualizing high-dimensional data using t-SNE,” *Journal of Machine Learning Research*, vol. 9, pp. 2579–2605, Nov 2008.
- [39] L. Van Der Maaten, “Accelerating t-SNE using tree-based algorithms,” *Journal of Machine Learning Research*, vol. 15, no. 1, pp. 3221–3245, Jan 2014.